Dipole Structure of Interannual Variations in Summertime Tropical Cyclone Activity over East Asia

JOO-HONG KIM AND CHANG-HOI HO

School of Earth and Environmental Sciences, Seoul National University, Seoul, South Korea

CHUNG-HSIUNG SUI

Institute of Hydrological Sciences, National Central University, Jung-li, Taiwan

SEON KI PARK

Department of Environmental Science and Engineering, Ewha Woman's University, Seoul, South Korea

(Manuscript received 30 August 2004, in final form 12 July 2005)

ABSTRACT

The present study examines variations in summertime (July–September) tropical cyclone (TC) activity over East Asia during the period 1951–2003. To represent TC activity, a total of 853 TC best tracks for the period were converted to TC passage frequencies (TPFs) within 5° × 5° latitude–longitude grids; TPFs are defined as the percentage values obtained by dividing the number of TC appearances in each grid box by the total number of TCs each year. Empirical orthogonal function analysis of the TPF showed three leading modes: two tropical modes that represent the long-term trend and the relationship with ENSO and one midlatitude mode that oscillates between south of Korea and southeast of Japan with an interannual time scale. The latter proved to be the most remarkable climatic fluctuation of summertime TC activity in the midlatitudes and is referred to as the East Asian dipole pattern (EADP) in this paper.

Anomalous atmospheric flows directly connected to the EADP are an enhanced anticyclonic (cyclonic) circulation centering around Japan when the TPF is high south of Korea (southeast of Japan), thereby showing an equivalent barotropic structure in the entire troposphere. This regional circulation anomaly varies in conjunction with the zonally oriented quasi-stationary Rossby wave train in the upper troposphere. This wave train is meridionally trapped in the vicinity of the summer-mean jet stream; therefore, the mean jet stream alters its internal meandering structure according to the phase of the wave train.

1. Introduction

Tropical cyclones (TCs) are one of the most destructive natural phenomena on earth. They are accompanied by strong winds and heavy rainfall, resulting in natural disasters such as high tides, flooding, and landslides. Each year many TCs—locally known as typhoons—hit East Asian countries, including China, Japan, and Korea. Although TCs become much weaker as they approach the cold oceans in the midlatitudes, they can still result in heavy rainfall and damaging wind gusts. For example, Typhoon Rusa—the 15th TC in 2002—struck Korea and caused tremendous nationwide damage with more than 220 people missing or dead, flash floods, and mudslides. The worst devastation occurred in the eastern coastal city of Gangneung, South Korea, which was stricken by the heaviest rainfall in the nation's history—870.5 mm of rainfall on a single day (31 August 2002).

Most TCs that enter the midlatitudes recurve around the edge of the North Pacific subtropical high (NPSH). One of the most pronounced variations in these TCs is the seasonal migration of the preferred recurving trajectory along with seasonal changes in large-scale circulations. Since the characteristics of the large-scale circulation can vary each year, the TC tracks also show significant interannual variation. Several previous studies have demonstrated that TC activity in the western North Pacific (WNP) would be modulated by various

Corresponding author address: Chang-Hoi Ho, School of Earth and Environmental Sciences, Seoul National University, San 56-1 Shillim-Dong, Gwanak-Gu, Seoul 151-742, South Korea.
E-mail: hoch@cpl.snu.ac.kr

TABLE 1. Monthly frequency of TCs that approached near Korea and Japan (entered the region 30°–40°N, 120°–140°E) during the period 1951–2003.

Month	Jan	Feb	Mar	Apr	May	Jun	Jul	Aug	Sep	Oct	Nov	Dec
TCs	1	0	0	3	11	37	85	123	96	43	14	1

atmospheric and oceanic phenomena that have time scales from intraseasonal to interdecadal: tropical intraseasonal oscillation (Hartmann et al. 1992; Liebmann et al. 1994), El Niño–Southern Oscillation (ENSO; Chan 1985, 2000; Chen et al. 1998; Chia and Ropelewski 2002; Lander 1994; Wang and Chan 2002), quasi-biennial oscillation (Chan 1995), and interdecadal variation of large-scale atmospheric circulations (Matsuura et al. 2003; Ho et al. 2004).

Among these, ENSO is generally regarded as the main phenomenon that influences the interannual variation of TC activity. The consensus is that the active genesis region of TC moves both eastward and equatorward, the life span increases, and TCs recurve more often and tend to recurve farther eastward during the warm phase of ENSO. In addition, during the El Niño years, many TCs move through the Pacific Ocean to the east of Japan due to the eastward shift in the preferred genesis location and the increased northward-steering flows (Wu and Wang 2004). Although it is obvious that ENSO is a major predictor of TC behavior in tropical and subtropical regions, it may not have a considerable impact on TC activity over midlatitude East Asian countries such as Korea and Japan (Saunders et al. 2000; Wu et al. 2004; Ho et al. 2005).

Continuous efforts have been made to characterize the interannual variation of overall seasonal TC activity (Chan 1985, 2000; Chan et al. 1998; Chan and Liu 2001; Chen et al. 1998; Camargo et al. 2004; and many others). Most of these studies focused on the variability of TC genesis, which is mainly related to the ENSO-related atmospheric–oceanic variability. To the best of our knowledge, thus far, no study has focused on the interannual variability of TC activity over midlatitude East Asia. As stated above, the influence of ENSO significantly weakens in this region; there may be distinctive large-scale climate variabilities other than ENSO that modulate the interannual variation of seasonal TC activity. Thus, the present study focuses on revealing the structure of the interannual variation of TC activity over East Asia, particularly near Korea and Japan, and understanding the relationship between this structure and large-scale atmospheric circulations.

Approximately 60% of the total annual TCs develop in the WNP from July to September; during this period, the passage of TCs through the regions near Korea and Japan is most frequent (Table 1). Therefore, in the present study, the analysis period is confined only to the boreal summer (July–September). This paper is arranged into six sections. In section 2, we describe the datasets and frequency distribution of TCs used in this study. The variability of TC activity and relevant large-scale atmospheric circulations are documented in sections 3 and 4, respectively. A more comprehensive dynamic interpretation of the relationship between TC activity and atmospheric circulations is discussed in section 5. The final section presents some concluding remarks.

2. Data

The present study utilizes the dataset of TC best tracks in the WNP that has been archived by the Regional Specialized Meteorological Centers–Tokyo Tropical Cyclone Center since 1951. Because this dataset includes only those TCs that have an intensity beyond that of a tropical storm, the term TC refers to both tropical storms ($V_{max} \geq 17$ m s^{-1}) and typhoons ($V_{max} \geq 33$ m s^{-1}) in this paper.

Since we studied 853 TCs that were formed during the boreal summer in the period 1951–2003, it would be appropriate to convert the 6-hourly latitude–longitude positions of TC tracks to gridded passage data to more comprehensively represent the variability of TC activity. Accordingly, each 6-hourly TC position is binned into the corresponding 5° × 5° latitude–longitude grid box. The same TC migrating in the same grid box is counted only once. The TC passage frequency (TPF) is defined as the percentage value obtained by dividing the number of TC appearances in each grid box by the total number of summertime TCs; the TPF is calculated for each summer. This percentage implies the probability of a TC appearing in each 5° × 5° grid box as it moves.

We also use the monthly mean horizontal winds and the geopotential heights reanalyzed by the National Centers for Environmental Prediction–National Center for Atmospheric Research (NCEP–NCAR) to characterize the related large-scale circulation patterns (Kalnay et al. 1996). These data are available on a 2.5° × 2.5° grid at standard pressure levels. The NCEP–NCAR reanalysis data were found to exhibit an unre-

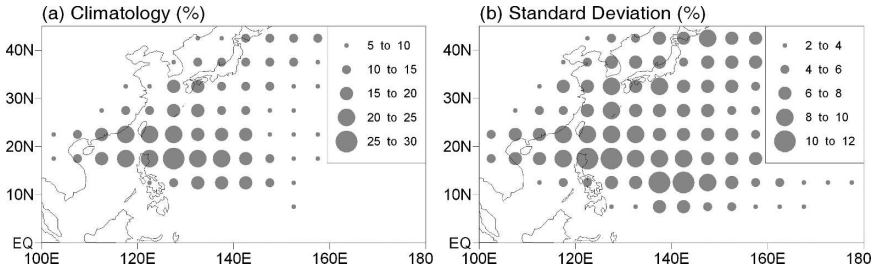

FIG. 1. Geographical distribution of the (a) summertime TPF and (b) its interannual standard deviation in each 5° × 5° grid area during the period 1951–2003.

alistic climatic jump around 1968 (Yang et al. 2002; Inoue and Matsumoto 2004). However, we believe that this error would not misguide us in interpreting the characteristics of large-scale circulations. In this study, the monthly climatology was first subtracted for each variable, and deviations from the climatology (i.e., anomalies) were mainly used.

3. East Asian dipole pattern

Over the WNP, the summer climatology of TC activities and their interannual standard deviation within each 5° × 5° grid box were obtained for the period 1951–2003 (Fig. 1). The interannual standard deviation was calculated based on the nine-point Gaussian digital filtered (weights of 0.01, 0.05, 0.12, 0.20, 0.24, 0.20, 0.12, 0.05, and 0.01) TPF in order to remove the possible influence of decadal–interdecadal variability. This filter removes variations longer than 10 yr and retains only the interannual variations (Gong and Ho 2003). Generally, TCs originating in the tropical Pacific tend to move north and northwestward around the periphery of the NPSH; hence, the TPF is high over the South China Sea, Philippine Sea, and southeast coast of China, as shown in Fig. 1a. The number of summertime TCs is approximately 16 in the WNP, and 15%–30% (two–five TCs) of the total occurrence enters the 5° × 5° grid boxes of the South China Sea, Philippine Sea, and southeast coast of China. The distribution of the standard deviation (Fig. 1b) shows features that are similar to those of the mean; however, noticeable discrepancies are found in the midlatitudes. Overall, the mean TPF gradually decreases from the Tropics to the midlatitudes, whereas the standard deviation even over the seas around Korea and Japan still shows high values in excess of 8%. These high values of standard deviation highlight the fact that the TC activity in the midlatitudes undergoes strong interannual variation.

To define the dominant modes of variation associated with the TPF, we applied the empirical orthogonal function (EOF) analysis to the entire 53-yr summertime TPF dataset. The EOF analysis is very popular as it is a convenient method for representing natural modes or patterns associated with the input data (North et al. 1982). It derives eigenvectors (i.e., EOFs, which are also known as principal components) and eigenvalues from a correlation or covariance matrix.

Figure 2 shows the three leading EOF modes that accounts for 15.2%, 10.7%, and 8.9% of the total variance. Considering the nature of diverse characteristics of the TC tracks, the total sum of the variance explained by these three modes can be regarded to account for a considerably large fraction of TC activity. In all EOF modes, there exist common characteristics wherein eigenvectors show standing oscillatory signals taking the shape of a dipole structure, and associated time series show long-term fluctuations as well as strong interannual variations. The first mode whose core of variability is located in the Tropics (12.5°N, 140°E) represents a long-term decreasing trend of TC activity in the Philippine Sea (Fig. 2a). Ho et al. (2004) previously mentioned that the decreasing trend is coherent with the decreasing trend of 850-hPa relative vorticity in the tropical WNP. Indeed, the decreasing vorticity in the lower troposphere contributes to unfavorable conditions for TC genesis.

The second mode also shows larger variability in the low latitudes that have a dipole pattern offshore from the Philippines and the open ocean east of the Philippines (Fig. 2b). This mode is apparently related to ENSO because it shows the east–west shift of TC genesis and subsequent tracks. To confirm this, we compared the time series with the Niño SST indices, which also proved that this mode becomes prominent during the strong warm/cold phase of ENSO (figure not shown).

While the first and second modes have a clear physical background, the third mode has not been previously documented from a physical viewpoint. This mode appears as an east–west dipole oscillation structure similar

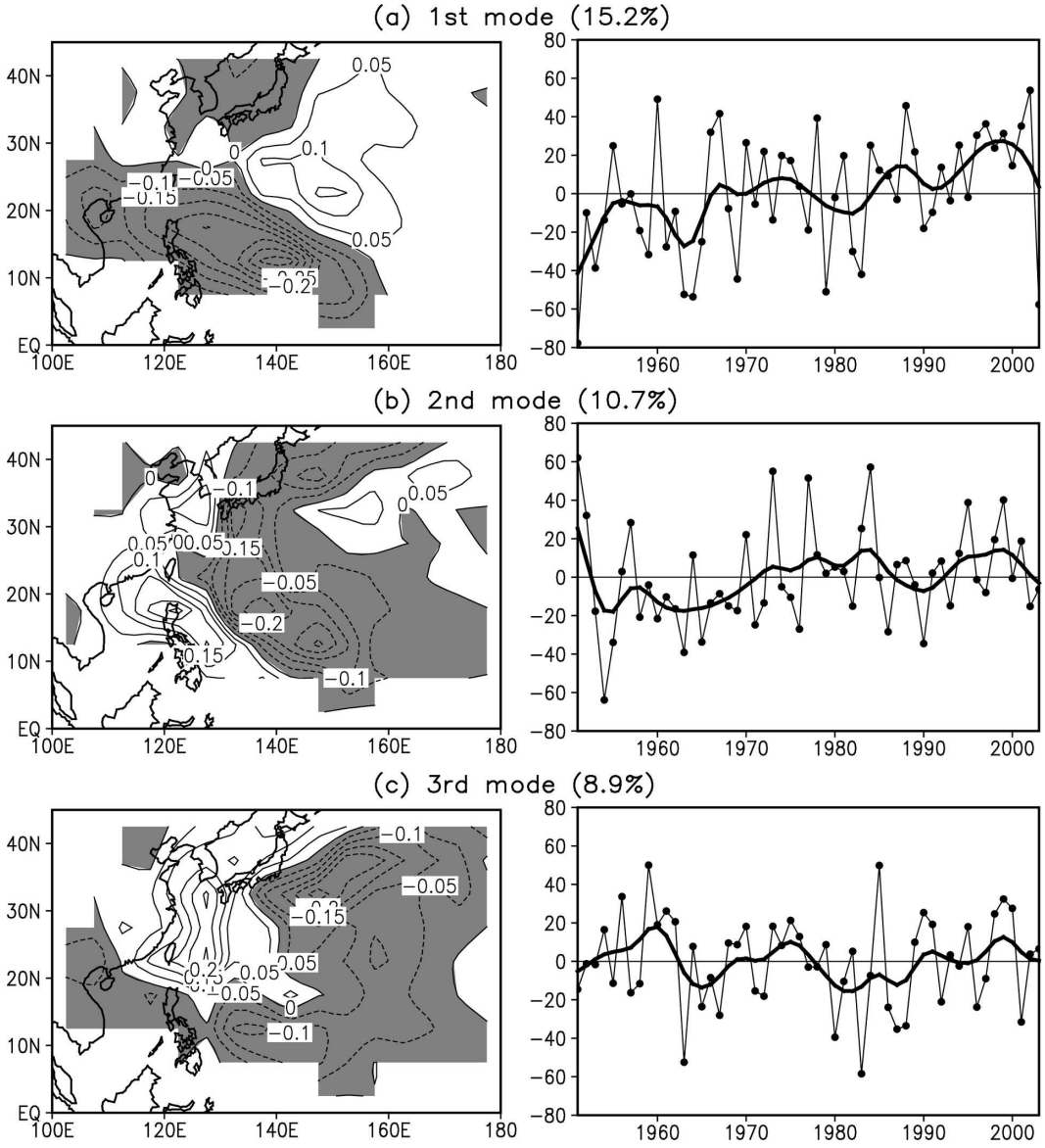

FIG. 2. (left) The three leading eigenvectors and (right) the associated time series of the summertime TPF during the period 1951–2003. The thick lines in the time series represent the low-pass-filtered values. The units are arbitrary: (a) first, (b) second, and (c) third modes.

to the spatial structure of the second mode; however, the centers of action are located more poleward (Fig. 2c). Two cores of the eigenvector are located in the East China Sea–South of Korea and southeast of Japan, and the associated time series does not show a long-term trend. Since this mode is the lowest mode whose cores of variability are located over midlatitude East Asia, we refer to this mode as the East Asian dipole pattern (EADP) in the present study.

Prior to the characterization of the EADP, a significant test of the EOF modes is required to ascertain whether each mode is distinct from the other modes (i.e., whether effective degeneracy occurs). North et al. (1982) mentioned that the geographical shape of an EOF shows large intersample variability when its associated eigenvalue is close to a neighboring one. They suggested a rule of thumb that considers EOFs as a probability distribution property estimated from a set of samples derived from a parent distribution. Thus, the rule of thumb is concerned with the extent to which the estimated EOFs accurately represent the true EOFs of the population. Based on such a rule of thumb, we schematically illustrate the first 10 eigenvalues with the standard errors due to sampling for each eigenvalue

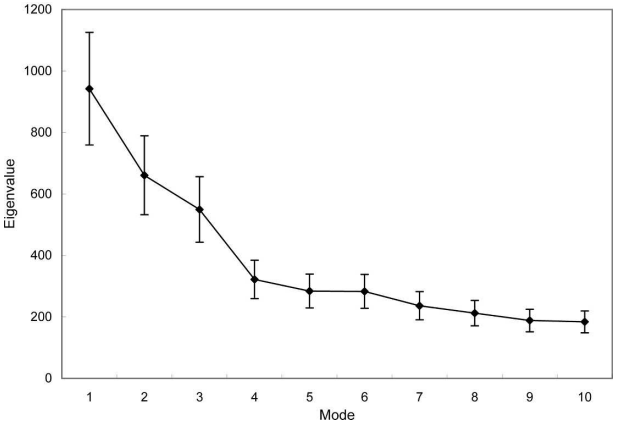

FIG. 3. Schematic diagram of the first 10 eigenvalues with the error bars on the eigenvalue estimates. The error bars represent the standard error (on standard deviation error due to sampling) for each eigenvalue.

(Fig. 3). As shown in this figure, the eigenvalues sharply decreased until the fourth EOF mode; thereafter, the dropping rate notably diminished (i.e., the three leading modes are thought to be isolated from the higher modes). However, the sampling errors of the second and third eigenvalues are sufficiently large to state that the sample eigenvectors associated with these modes are a random mixture of the true eigenvectors. Based on this point, the existence of the EADP could be disputed. However, since the second mode is physically explained by the ENSO-related variations despite the effective degeneracy, the third mode may also have both/either its own physical meaning and/or just the impact of ENSO; otherwise, neither of these. Complementarily, we performed the EOF analysis over the domain north of 20°N (figure not shown). The spatial structure of the first mode was identical to that of the third mode in the former EOF analysis with an explained variance of 15%. The second mode (~10.3%) shows a tripole structure similar to the variability in the midlatitudes of the second mode EOF shown in Fig. 2b. This result supports the possible existence of the EADP, which explains the largest fraction of the interannual variations in summertime TC tracks over midlatitude East Asia.

The relatively low value (~8.9%) of the explained variance corresponding to the EADP requires examination of whether the oscillatory signal is really shown in the raw data. Two core regions were selected in this case: one is south of Korea (30°–35°N, 120°–135°E) and the other is southeast of Japan (30°–35°N, 140°–155°E). The time series of the TPFs in these two boxes are presented in Fig. 4. Note that the two time series show an apparent inverse relationship (i.e., the TPF south of Korea increases while that southeast of Japan decreases and vice versa). The correlation coefficient for the analysis period is −0.52, which is significant at the 99% confidence level. It is also interesting to note that the inverse relationship becomes rather strong after the mid-1970s. A possible cause may be found in the interdecadal variability in the WNP during the same period (Chang et al. 2000; Gong and Ho 2002; Hu 1997); how-

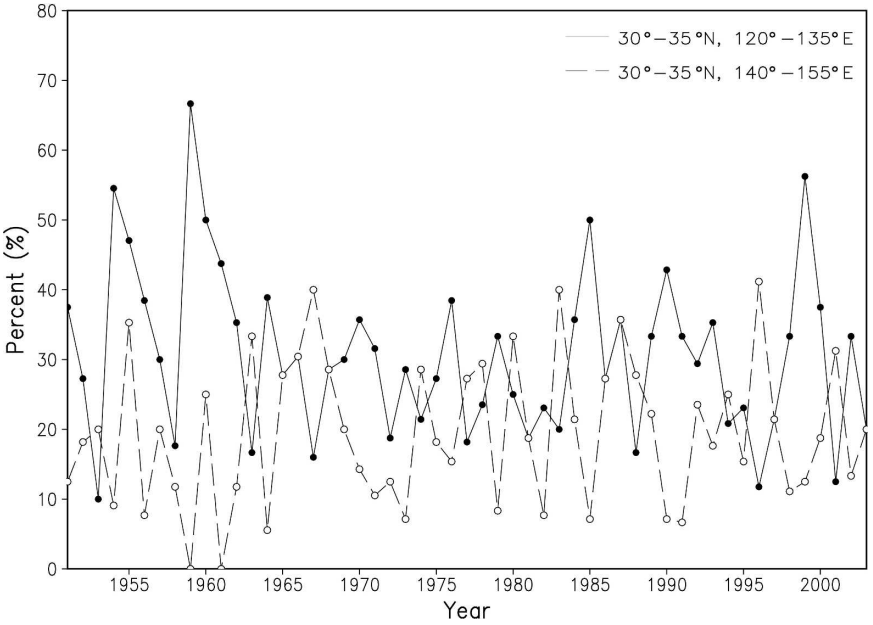

FIG. 4. Time series of the TPF for south of Korea (30°–35°N, 120°–135°E, solid line) and for southeast of Japan (30°–35°N, 140°–155°E, dotted line) for the period 1951–2003.

ever, examining this is beyond the scope of the present paper.

In the following, we will use two time series instead of the time series of the third mode, by constructing the composite large-scale environmental fields associated with the EADP. Prior to proceeding, the coherence between the time series of the third mode and those of the two selected regions should be examined to ensure the robustness of current results, irrespective of which is used. Linear correlation between the time series of an East Asian dipole index (calculated by subtracting the TPF for the region south of Japan from the TPF for the region south of Korea) and the time series of the third EOF mode is more than 0.8, which is significant at the 99% confidence level. A high correlation between the two time series will ensure consistency.

4. Characteristics of large-scale atmospheric circulation

To examine the distribution of large-scale environmental flows connected to the EADP, we adopt a composite method based on the time series of the TPF south of Korea and southeast of Japan. The tropospheric layer mean winds (TLMWs) are regarded as the environmental steering currents that explain the majority of TC movements (George and Gray 1976; Chan and Gray 1982). The TLMWs are defined as

$$\mathbf{V}_{\text{trop}} = \frac{1}{p_b - p_t} \int_{p_t}^{p_b} \mathbf{V}\, dp,$$

where p_b is taken as 850 hPa and p_t as 200 hPa. The years of high/low TPF are selected based on significant TPF anomalies (i.e., the TPF anomalies are greater/smaller than one standard deviation from the climatology). South of Korea, the high TPF years include 1954, 1959, 1960, 1961, 1985, 1990, and 1999, while the low TPF years include 1953, 1958, 1963, 1967, 1972, 1977, 1981, 1988, 1996, and 2001. Southeast of Japan, the high TPF years include 1963, 1966, 1967, 1980, 1983, 1987, 1996, and 2001, while the low TPF years include 1954, 1956, 1959, 1961, 1964, 1973, 1979, 1982, 1985, 1990, and 1991.

The differences in the TLMWs between the high TPF years and the low TPF years over the two selected regions are shown in Fig. 5. The gray shaded areas represent statistical significance at the 95% confidence level. Characteristic anomalous patterns of TLMWs related to the EADP are zonally oriented chains of anomalous anticyclonic and cyclonic circulations that straddle the Asian continent and the North Pacific Ocean (Fig. 5a). The horizontal extent of anomalous circulation cells is approximately 3000–4000 km, which is a typical length scale for synoptic-scale wave disturbances. When the TPF is high south of Korea, two cyclonic circulation anomalies are located in north China and south of the Kamchatka Peninsula and a strong anticyclonic circulation anomaly is dominant over Korea and Japan. Associated with these anomalous circulations, strong southerly (northerly) winds prevail over Korea (east of Japan). At the same time, the easterly anomalies prevail over 20°N, 140°–170°E. These anomalous steering currents act to prohibit TCs from sharp recurving; therefore, the TCs are more likely to be steered toward Korea. On the other hand, when the TPF is high southeast of Japan, the composite pattern showed completely contrasting features (Fig. 5b). The strongest circulation anomaly is also located near Korea and Japan. Thus, the EADP is mainly controlled by the seasonal-mean large-scale circulation anomalies near Japan, which is a constituent of zonally oriented chains of circulation anomalies in the midlatitudes.

Since the TLMWs are vertically averaged values (i.e., single layer variables), there may be a barotropic assumption when we relate the EADP to the zonally oriented chains of circulation anomalies in the TLMWs. To ascertain whether the anomalous circulations within the entire troposphere actually have a barotropic structure, we illustrate the zonal and meridional vertical cross sections of the geopotential heights in Fig. 6. Composite differences in the geopotential heights were averaged between the latitudes 30° and 50°N (Figs. 6a,b) between the high TPF years and the low TPF years with respect to each selected region. This shows that alternation of highs and lows is developed through the tropospheric deep layer. This is consistent with the TLMWs (Fig. 5), showing the same phase in the upper troposphere and lower troposphere (i.e., an equivalent barotropic structure). The meridional vertical cross sections averaged between the longitudes 125° and 150°E (Figs. 6c,d) also show the same phase structure vertically from the troposphere to the stratosphere, except for the lower-tropospheric region northward of 40°N, with a slight northward tilt in the midlatitudes. In the Tropics, an opposite phase is prominent through the deep layer. Thus, we may deduce that meridional mass exchange between the Tropics and extratropics is also possibly related to the EADP.

Figure 7 shows the linear correlation between the time series of the TPF in each selected region and the large-scale environmental fields. Overall features confirm the significance of the composite fields with respect to the extreme phase. For the time series of the TPF south of Korea, the TLMWs near Korea have the best correlation values of more than 0.5. Thus, the southerly winds associated with the anticyclone center-

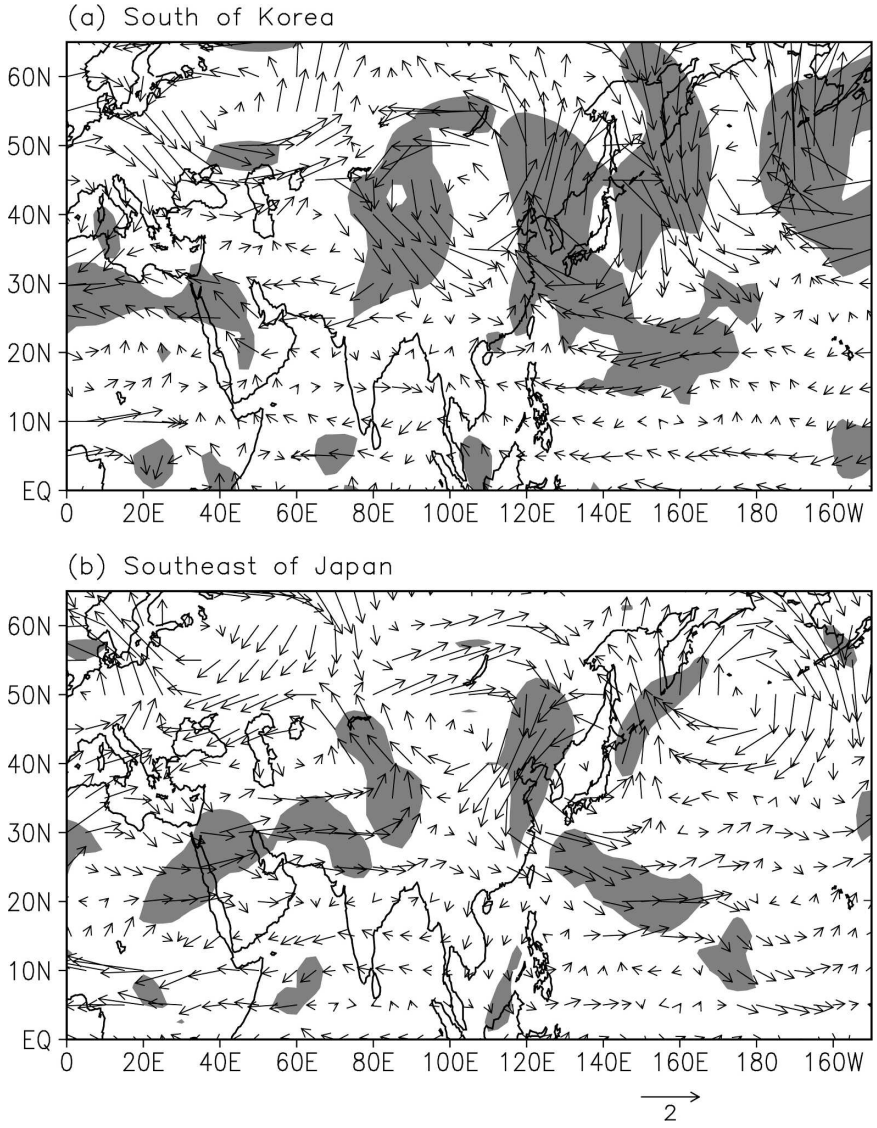

FIG. 5. Difference of the TLMWs in the troposphere (850–200 hPa) between the high TPF years composite and the low TPF years composite for (a) south of Korea and for (b) southeast of Japan. Shaded areas are statistically significant at the 95% confidence level using the two-sided Student's t test. Vector unit is m s^{-1}.

ing around Japan are most significantly related to the TPF south of Korea. For the time series of the TPF southeast of Japan, overall maximum correlation values are slightly lower than those for south of Korea, except for the zonal winds. Even though the correlation patterns may be weak to a greater extent, two counterpatterns evidently showed an opposite phase of climatic state.

In the correlation maps, we selected some areas that show a high correlation to generate area-mean atmospheric indices. The areas selected according to the large-scale environmental factors are presented in Table 2. Most of the correlations between the time series of the TPF in each selected region and the large-scale circulation indices are statistically significant, except for those between the time series of the TPF southeast of Japan and the 500-hPa geopotential height index. As shown in the correlation map, the v component of the TLMWs averaged over 20°–50°N, 115°–135°E shows the most significant correlation with the time series of the TPF. The correlation coefficient between the time series of the TPF south of Korea (southeast of Japan) and the meridional wind index is 0.63 (−0.44), which is significant at the 99% confidence level. The stronger connection with the meridional wind index in comparison with the zonal wind index

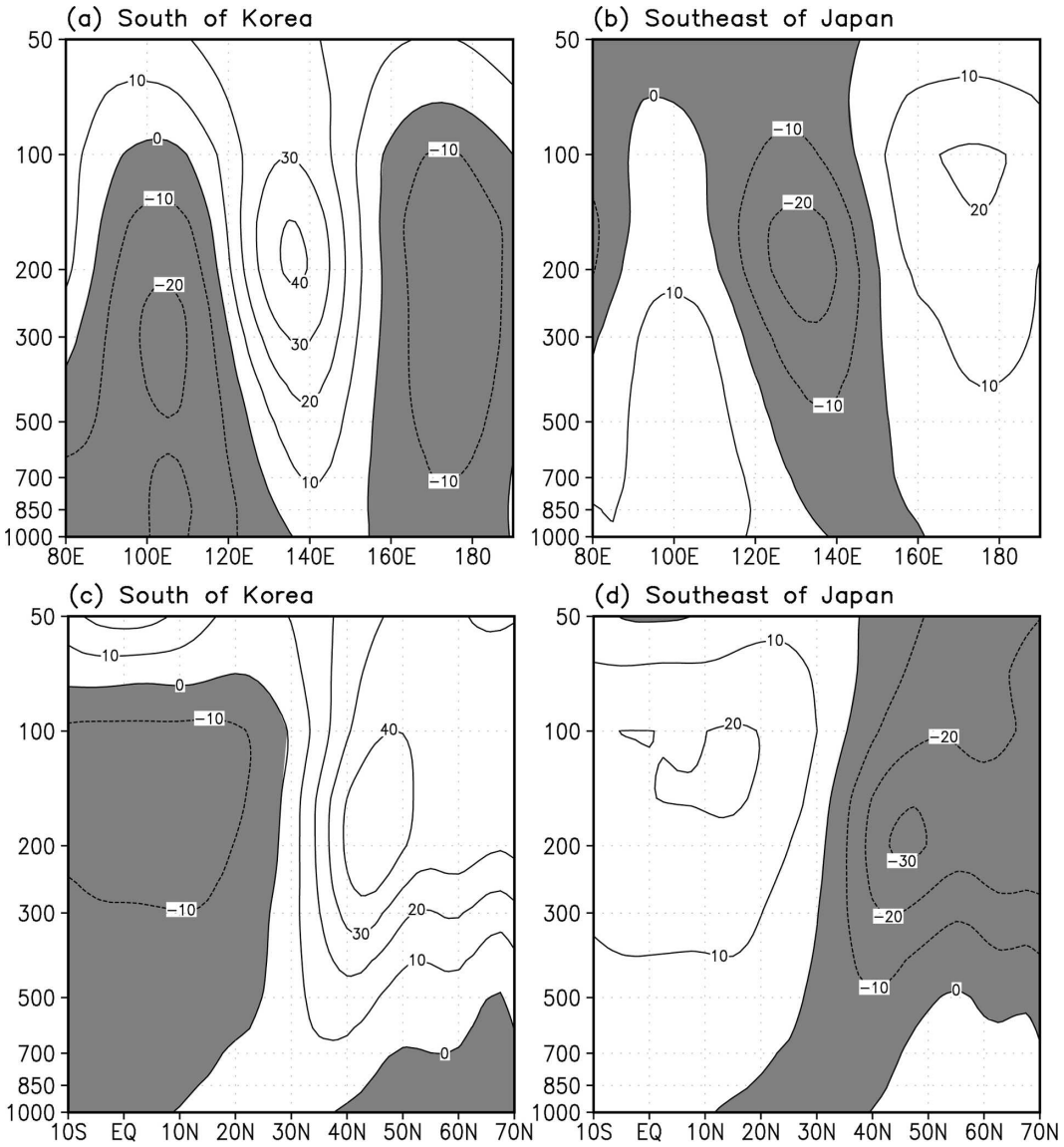

FIG. 6. Same as in Fig. 5, except for (a), (b) longitude–height cross section of the geopotential heights (in m) averaged between the latitudes 30° and 50°N and (c), (d) latitude–height cross section of those averaged between the longitudes 125° and 150°E.

implies that the zonally asymmetric component plays a more crucial role in inducing the EADP than the zonal mean component. In other words, more weight is given to shorter zonal scales (smaller scales) in relation to the EADP.

5. Discussion

In this section, we present a more comprehensive discussion of the dynamical structure related to the EADP and evaluate the effect of the location of genesis and the variation of the NPSH on the pattern.

a. Dynamical structure

The EADP discussed thus far, which represents the interannual variations of summertime TC activity over midlatitude East Asia, reveals zonally oriented chains of anomalous anticyclonic and cyclonic circulations spanning from Arabia to the North Pacific Ocean (i.e., a meridionally trapped teleconnection wave train). With regard to the wave train, the development/decline of the anomalous anticyclonic cell centering around Japan is directly correlated with the oscillatory phase of the EADP.

For further consideration of the three-dimensional

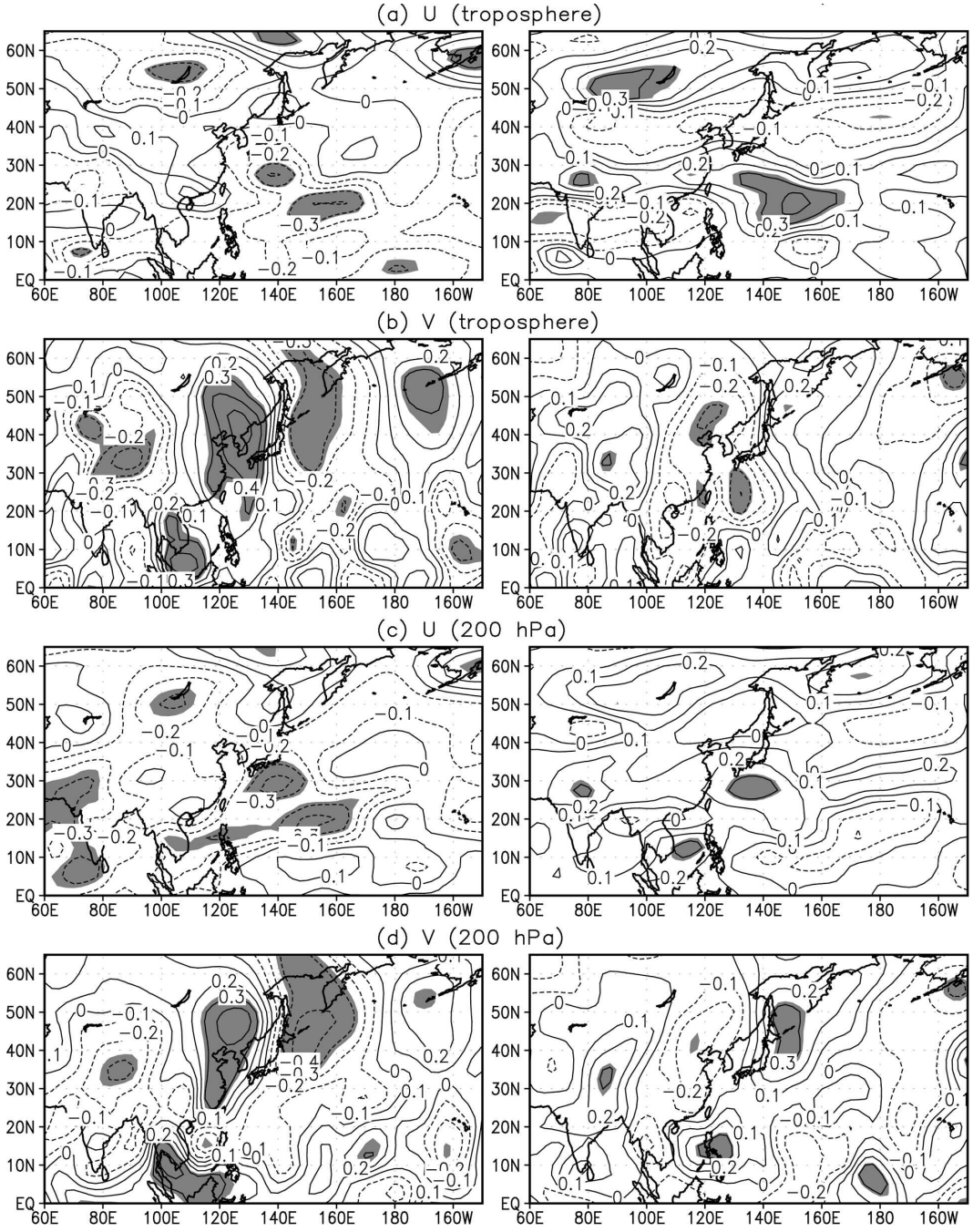

FIG. 7. One-point correlations between the time series of the TPF in each box and (a) the tropospheric layer-mean u, (b) the tropospheric layer-mean v, (c) the 200-hPa u, and (d) the 200-hPa v for (left) south of Korea and (right) southeast of Japan. Shaded areas are statistically significant at the 95% confidence level using the two-sided Student's t test.

structure associated with the EADP, we have shown the anomalous fields of the horizontal winds and the geopotential heights as well as the mean fields of the zonal winds in the upper troposphere (200 hPa) and the lower troposphere (850 hPa) in Fig. 8. For brevity, we have displayed only the fields that are related to the difference between the high TPF years and the low TPF years in the region south of Korea.

At 200 hPa (Fig. 8a), clear zonally oriented perturbation chains span the entire domain from Europe to

TABLE 2. Correlations between the atmospheric circulation indices and the time series of the TPF south of Korea (southeast of Japan).

Indices	South of Korea	Southeast of Japan
$U_{trop}1$ (15°–25°N, 140°–170°E)	−0.39*	0.42*
$U_{trop}2$ (25°–30°N, 130°–145°E)	−0.36*	0.31**
V_{trop} (20°–50°N, 115°–135°E)	0.63*	−0.44*
U_{200} (25°–35°N, 125°–150°E)	−0.38*	0.33**
V_{200} (40°–50°N, 140°–160°E)	−0.46*	0.34**

* The 99% confidence level is ±0.35.
** The 95% confidence level is ±0.27.

the Gulf of Alaska, similar to the TLMWs shown in Fig. 4. The latitudinal location of the upper-tropospheric wave train shifts slightly northward compared with that of the TLMWs, which is consistent with the poleward tilt shown in Fig. 6c. The thick solid (dashed) line with red (blue) color represents the location of the summer-mean jet stream when the TPF is high (low). The wave train follows the axis of the mean jet stream. Two mean jets show similar latitudinal location with respect to the different phase of the EADP; however, their meandering structure appears in an out-of-phase relationship, which is definitely due to the phase difference of the

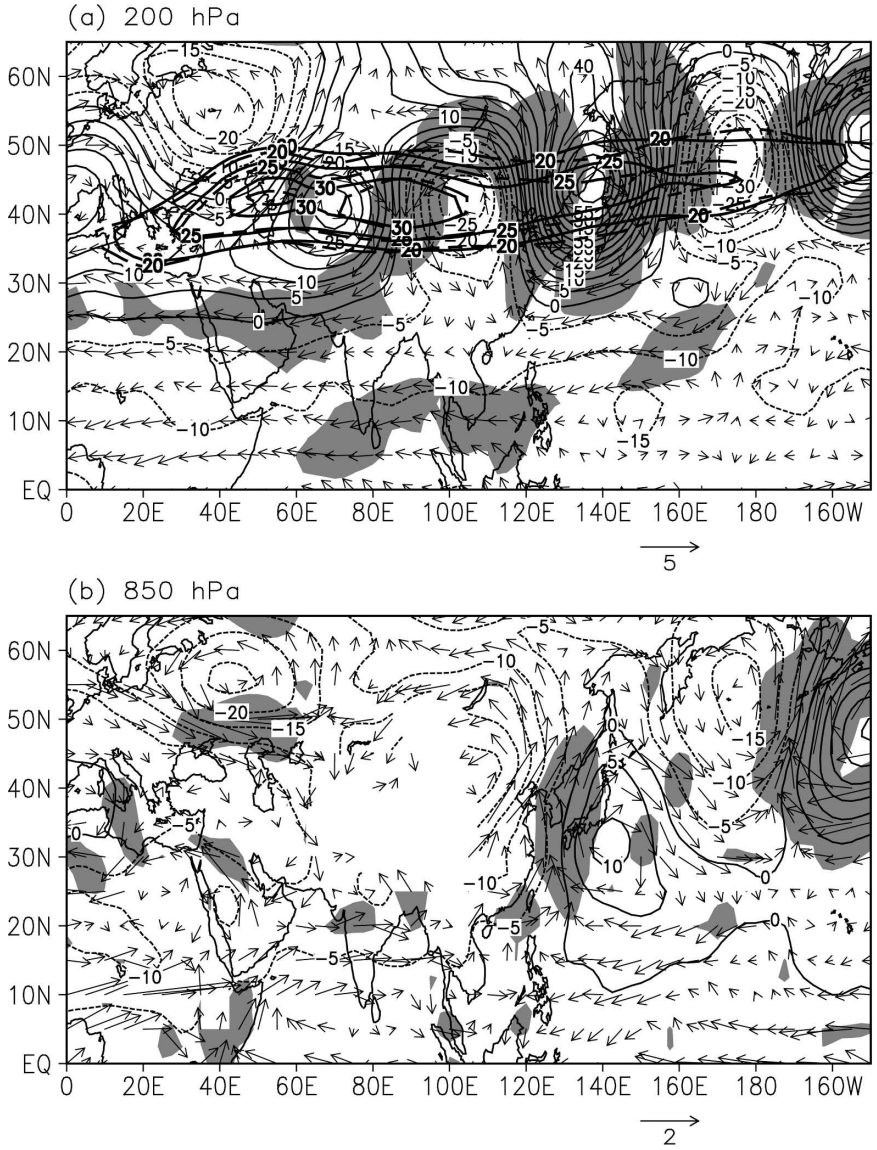

FIG. 8. Same as in Fig. 5, except for the difference in the horizontal winds and the geopotential heights at (a) 200 and (b) 850 hPa. Additionally, the mean u at 200 hPa when the TPF is high (low) south of Korea is represented by thick solid (dashed) line. Shaded areas representing the horizontal wind fields are significant.

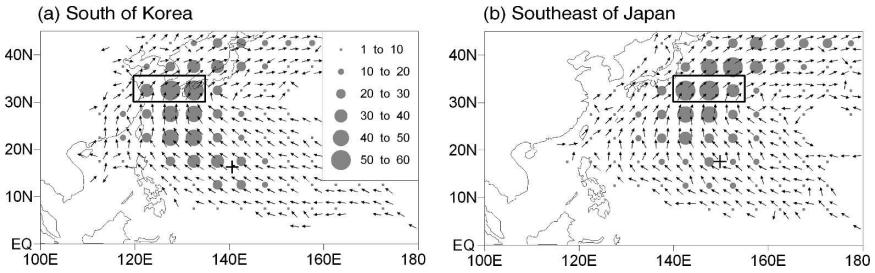

FIG. 9. The backtracked TPF with the 5° × 5° latitude–longitude grid box and the mean direction with the 2.5° × 2.5° latitude–longitude grid box of summertime TCs that pass over (a) south of Korea and (b) southeast of Japan. The plus sign (+) indicates the mean genesis position.

quasi-stationary Rossby wave train following them. If we discuss this in a more regional context, the axis of the jet stream shifts northward (southward) when the TPF is high south of Korea (southeast of Japan); therefore, the westerlies near 30°N are significantly weakened (strengthened).

The role of time mean jets on the behavior of low-frequency disturbances has been previously reported in many previous studies (Hoskins and Ambrazzi 1993; Branstator 2002; Watanabe 2004; and many others). Both observational and barotropic modeling studies have suggested that the low-frequency perturbations will tend to be meridionally trapped where the jet stream is centered, indicating that the disturbances near the jet core are refracted toward the core. This implies that the jet acts as a waveguide. Although most papers have focused on the wintertime activity, the same internal dynamics of the time mean jets may be proposed in the light of the current observations during the summertime. Lau et al. (2000) mentioned that the dynamics of the anomalous circulation over the Asian continent during the boreal summer is underpinned by barotropic interaction with the climatological westerly jet, which supports the above-mentioned argument.

At 850 hPa (Fig. 8b), strong southerly winds related to the anomalous anticyclonic circulation southeast of Japan are dominant over the East China Sea through Korea, suggesting an expansion of the NPSH. The wave train pattern shows the same phase as the upper troposphere even though it weakens, which again supports an equivalent barotropic structure.

b. Genesis location and the NPSH

The preferential zone of TCs that recurve into midlatitudes may be related to the longitudinal shift of genesis locations. Figure 9 shows the TPFs that are constituted by back tracking the TCs that pass through the two core regions. This is thought to be representative of the average impact of the genesis location on the EADP. The number of TCs passing over south of Korea (southeast of Japan) is 234 (155). The difference in the mean genesis locations is approximately 9° longitudinally. Since ENSO has been known to have the most significant impact on the longitudinal shift of TC genesis locations (Lander 1994; Chen et al. 1998; Chan 2000; Wang and Chan 2002), this slight difference in longitudinal mean location suggests a marginal effect on ENSO. However, it appears not to be very effective for the EADP since the distribution of the locations of genesis is too scattered to have any statistical significance. We also ascertained the linear correlation between the EADP and the Niño SST indices. The result shows that the SST time series leads the TPF time series by 1 or 2 months in both the selected core regions. However, all simultaneous and lag correlation values also show marginal relationships, and this fact supports the weak impact of ENSO on the EADP.

In the figure, we also show the arrows that indicate the mean direction of TCs in each grid area. The TCs passing over south of Korea generally recurve around 30°N, and those passing over southeast of Japan generally recurve at a slightly lower latitude. The difference in the recurving latitude is consistent with the changes in atmospheric flows over East Asia, as discussed in this study. As shown in Fig. 8b, the anomalous 850-hPa circulation cell centered southeast of Japan is associated with the march/retreat of the NPSH into/from midlatitude East Asia. Thus, it is reasonable to state that the significant wind anomalies in the subtropical WNP are due to the variation in a sphere of influence of the NPSH that is influenced by the circulation anomalies spanning from Arabia to the North Pacific Ocean, thereby causing the difference in the recurving latitude.

6. Concluding remarks

In the present study, we examined the variation of summertime TC activity over the WNP during the pe-

riod 1951–2003. Application of the EOF analysis to the 53-yr summertime TPF data successfully separated the leading orthogonal physical modes associated with climate fluctuation of the large-scale atmospheric circulations. The centers of variability presented in the first and second EOFs are placed in the Tropics and subtropics, representing the long-term trend and the relationship with ENSO, respectively. However, the third EOF has oscillation centers over midlatitude East Asia; one is over south of Korea and the other is over southeast of Japan. This east–west oscillatory mode, the so-called EADP, emerges as the most notable variation in summertime TC tracks passing midlatitude East Asia.

The most remarkable structure of the large-scale anomalous circulation associated with the EADP is the zonally oriented quasi-stationary Rossby wave train spanning from Arabia to the North Pacific Ocean. Each anomalous circulation cell has a horizontal scale of 3000–4000 km. The strongest variation is the alternation of the circulation anomalies centering around Japan, and the most significantly correlated variable is the meridional winds near the Korean peninsula. The wave train becomes very clear in the upper troposphere and is meridionally trapped in the vicinity of the summer-mean jet stream, indicating the jet waveguide.

This study also supports the claim that TC tracks are significantly controlled by the seasonal-mean regional atmospheric circulation. If we consider a specific track of TC, we should be concerned with various aspects of the phenomenon, such as external, internal, and interactive dynamics of TCs (Wang et al. 1998). However, once we shift to a climatic viewpoint, involving consideration of the interannual or interdecadal variation and climate change, the time-mean large-scale steering flows become a major factor in determining the TC tracks. This is because the transient TCs are substantially removed from the time-mean environmental flows.

Acknowledgments. This study was performed for the Research and Development Programs on Meteorology and Seismology funded by the Korean Meteorological Administration. C.-H. Sui acknowledges the support received by NSC93-2111-M-008-002. The authors thank two anonymous reviewers. Their careful review and helpful suggestions led to the improvement of this paper.

REFERENCES

Branstator, G., 2002: Circumglobal teleconnections, the jet stream waveguide, and the North Atlantic Oscillation. *J. Climate,* **15,** 1893–1910.

Camargo, S. J., A. W. Robertson, S. J. Gaffney, and P. Smyth, 2004: Cluster analysis of western North Pacific tropical cyclone tracks. *Extended Abstracts*, *26th Conf. on Hurricanes and Tropical Meteorology*, Miami, FL, Amer. Meteor. Soc., 10A.7. [Available online at http://ams.confex.com/ams/26HURR/techprogram/paper_75358.htm.]

Chan, J. C. L., 1985: Tropical cyclone activity in the Northwest Pacific in relation to the El Niño/Southern Oscillation phenomenon. *Mon. Wea. Rev.,* **113,** 599–606.

——, 1995: Tropical cyclone activity in the western North Pacific in relation to the stratospheric quasi-biennial oscillation. *Mon. Wea. Rev.,* **123,** 2567–2571.

——, 2000: Tropical cyclone activity over the western North Pacific associated with El Niño and La Niña events. *J. Climate,* **13,** 2960–2972.

——, and W. M. Gray, 1982: Tropical cyclone movement and surrounding flow relationships. *Mon. Wea. Rev.,* **110,** 1354–1374.

——, and K. S. Liu, 2001: Improvements in the seasonal forecasting of tropical cyclone activity over the western North Pacific. *Wea. Forecasting,* **16,** 491–498.

——, J. Shi, and C. Lam, 1998: Seasonal forecasting of tropical cyclone activity over the western North Pacific and the South China Sea. *Wea. Forecasting,* **13,** 997–1004.

Chang, C.-P., Y. Zhang, and T. Li, 2000: Interannual and interdecadal variations of the East Asian summer monsoon and tropical Pacific SSTs. Part I: Roles of the subtropical ridge. *J. Climate,* **13,** 4310–4325.

Chen, T.-C., S.-P. Weng, N. Yamazaki, and S. Kiehne, 1998: Interannual variation in the tropical cyclone formation over the western North Pacific. *Mon. Wea. Rev.,* **126,** 1080–1090.

Chia, H.-H., and C. F. Ropelewski, 2002: The interannual variability in the genesis location of tropical cyclones in the northwest Pacific. *J. Climate,* **15,** 2934–2944.

George, J. E., and W. M. Gray, 1976: Tropical cyclone motion and surrounding parameter relationships. *J. Appl. Meteor.,* **15,** 1252–1264.

Gong, D.-Y., and C.-H. Ho, 2002: Shift in the summer rainfall over the Yangtze River valley in the late 1970s. *Geophys. Res. Lett.,* **29,** 1436, doi:10.1029/2001GL014523.

——, and ——, 2003: Arctic oscillation signals in the East Asian summer monsoon. *J. Geophys. Res.,* **108,** 4066, doi:10.1029/2002JD002193.

Hartmann, D. L., M. L. Michelsen, and S. A. Klein, 1992: Seasonal variations of tropical intraseasonal oscillations: A 20-25-day oscillation in the western Pacific. *J. Atmos. Sci.,* **49,** 1277–1289.

Ho, C.-H., J.-J. Baik, J.-H. Kim, D.-Y. Gong, and C.-H. Sui, 2004: Interdecadal changes in summertime typhoon tracks. *J. Climate,* **17,** 1767–1776.

——, J.-H. Kim, H.-S. Kim, C.-H. Sui, and D.-Y. Gong, 2005: Possible influence of the Antarctic Oscillation on tropical cyclone activity in the western north Pacific. *J. Geophys. Res.,* **110,** D19104, doi:10.1029/2005JD005766.

Hoskins, B. J., and T. Ambrazzi, 1993: Rossby wave propagation on a realistic longitudinally varying flow. *J. Atmos. Sci.,* **50,** 1661–1671.

Hu, Z.-Z., 1997: Interdecadal variability of summer climate over East Asia and its association with 500 hPa height and global sea surface temperature. *J. Geophys. Res.,* **102,** 19 403–19 412.

Inoue, T., and J. Matsumoto, 2004: A comparison of summer sea level pressure over East Eurasia between NCEP-NCAR reanalysis and ERA-40 for the period 1960-99. *J. Meteor. Soc. Japan,* **82,** 951–958.

Kalnay, E., and Coauthors, 1996: The NCEP/NCAR 40-Year Reanalysis Project. *Bull. Amer. Meteor. Soc.,* **77,** 437–471.

Lander, M. A., 1994: An exploratory analysis of the relationship between tropical storm formation in the western North Pacific and ENSO. *Mon. Wea. Rev.,* **122,** 636–651.

Lau, K.-M., K.-M. Kim, and S. Yang, 2000: Dynamical and boundary forcing characteristics of regional components of the Asian summer monsoon. *J. Climate,* **13,** 2461–2482.

Liebmann, B., H. H. Hendon, and J. D. Glick, 1994: The relationship between tropical cyclones of the western Pacific and Indian Oceans and the Madden-Julian Oscillation. *J. Meteor. Soc. Japan,* **72,** 401–411.

Matsuura, T., M. Yumoto, and S. Iizuka, 2003: A mechanism of interdecadal variability of tropical cyclone activity over the western North Pacific. *Climate Dyn.,* **21,** 105–117.

North, G. R., T. L. Bell, R. F. Cahalan, and F. J. Moeng, 1982: Sampling errors in the estimation of empirical orthogonal functions. *Mon. Wea. Rev.,* **110,** 699–706.

Saunders, M. A., R. E. Chandler, C. J. Merchant, and F. P. Roberts, 2000: Atlantic hurricanes and NW Pacific typhoons: ENSO spatial impacts on occurrence and landfall. *Geophys. Res. Lett.,* **27,** 1147–1150.

Wang, B., and J. C. L. Chan, 2002: How strong ENSO events affect tropical storm activity over the western North Pacific. *J. Climate,* **15,** 1643–1658.

——, R. Elsberry, Y. Wang, and L. Wu, 1998: Dynamics in the tropical cyclone motion: A review. *Chinese J. Atmos. Sci.,* **22,** 535–547.

Watanabe, M., 2004: Asian jet waveguide and a downstream extension of the North Atlantic Oscillation. *J. Climate,* **17,** 4674–4691.

Wu, L., and B. Wang, 2004: Assessing impacts of global warming on tropical cyclone tracks. *J. Climate,* **17,** 1686–1698.

Wu, M. C., W. L. Chang, and W. M. Leung, 2004: Impacts of El Niño–Southern Oscillation events on tropical cyclone landfalling activity in the western North Pacific. *J. Climate,* **17,** 1419–1428.

Yang, S., K.-M. Lau, and K.-M. Kim, 2002: Variations of the East Asian jet stream and Asian–Pacific–American winter climate anomalies. *J. Climate,* **15,** 306–325.